Supplementary Information

Metal Ion-Selective Chiral Gelation of Mannose-Grafted Polyoxometalate Cluster

Mingfeng Wei, Lei Wang, Bao Li* and Lixin Wu*

State Key Laboratory of Supramolecular Structure and Materials, College of Chemistry, Jilin University, Changchun 130012, P. R. China.

**E-mail: wulx@jlu.edu.cn, libao@jlu.edu.cn*

Contents

S1. Materials

The general chemicals, D-Mannose, 4-dimethylaminopyridine [DMAP], 2-bromoethanol, Boron trifluoride etherate [$BF_3{\cdot}O(C_2H_5)_2$], sodium azide, sodium methanolate, N-ethoxycarbonyl-2-ethoxy-1,2-dihydroquinoline (EEDQ), 2-propynylamine, succinic anhydride, amberlite (IR 120 H^+), Na_2SO_4, NaCl, $NaClO_4$, $ZnSO_4{\cdot}7H_2O$, NH_4Cl and common organic solvents were purchased from Sinopharm Chemical Reagent Co., Ltd. All the commercially available products were used without further purification. All the solvents were analytical grade and used as received. Doubly distilled water was used throughout the experiments.

S2. Measurements

^1H NMR, 2D COSY and ^{13}C NMR spectra were recorded on a Bruker Avance 500 MHz spectrometer by using tetramethylsilane (TMS) as internal reference (s= siglet, br= broad, d =doublet, t= triplet, q= quartet, m= multiplet). FT-IR spectra (KBr pellet) were collected on a Bruker Vertex 80 V spectrometer equipped with DTGS detector (32 scans) at a resolution of 4 cm^{-1}. Organic elemental analyses (C, H, N) were carried out on a Vario micro cube from Elementar. Scanning electronic microscopic (SEM) measurement was performed on a JEOL JSM-6700F field emission scanning electron microscope. Atomic force microscopic (AFM) images were taken with a Dimension FastScanTM atomic force microscope from Bruker under ambient conditions. X-ray diffraction (XRD) data were recorded on a Rigaku SmartLab 3 X-ray diffractometer using Cu Kα1 radiation at wavelength of 1.542 Å. X-ray photoelectron spectra was carried out on an ESCALAB 250 spectrometer from Thermo with a monochromic X-ray source (Al Ka line, 1,486.6 eV) and the charging shift was corrected by the binding energy of C (1s) at 285.0eV. GC mass spectra were carried out by ion trap gas chromatography (GC) mass spectrometer (Thermo Fisher-ITQ1100, USA) with electron impact (EI) ionization mode. Rheology measurements were executed on a Discovery Hybrid Rheometer (TA HR-1, USA).

S3. Preparation of supramolecular hydrogels

SMMM (10.0 mg, 5 μmol) and $CuSO_4$ (1.25 mg, 5 μmol) at 1:1 molar ratio was mixed in 300 μL of H_2O. After 2 h sonication of the solution the supramolecular hydrogel formed for structural measurements and post-treatment. The dry gel is insoluble in dichloromethane, so it is dispersed in dichloromethane to observe the assembly structure. For other gel samples prepared from others metal ions, $FeSO_4$, $CoSO_4$, $NiSO_4$, and $AgNO_3$ were used following the same methods under the same concentrations.

S4. Synthesis of ionic complex (SMMM)

The synthesis of the ionic complex follows the route shown in Fig. S1.

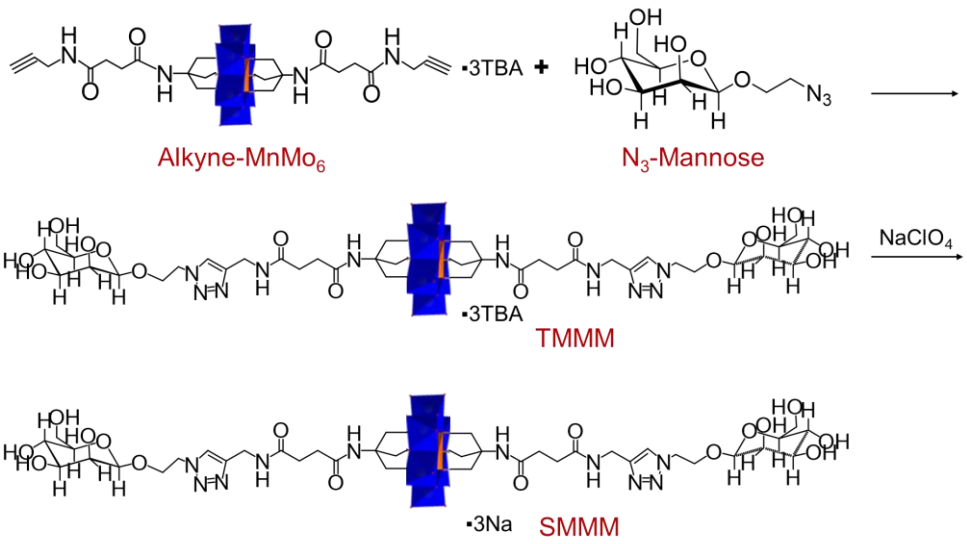

Fig. S1 Synthetic route of ionic complex molecule SMMM.

$[N(C_4H_9)_4]_3\{MnMo_6O_{18}[(OCH_2)_3CNHCO(CH_2)_2CONHCH_2(C_9H_{16}O_6N_3)_2]_2\}$ (TMMM). $[N(C_4H_9)_4]_3\{MnMo_6O_{18}[(OCH_2)_3CNHCO(CH_2)_2CONHCH_2CCH]_2\}$ (Alkyne-$MnMo_6$), which synthesis was followed by similar procedures reported in literature[1], (0.25 g, 0.1 mmol, 1 eq) was dissolved in DMF (10 mL) while β-D-Mannopyranoside-2-azidoethyl (N_3-Mannose), which synthesis was followed by similar procedures reported in literature[2], (0.14 g, 0.56 mmol, 5 eq) was dissolved in H_2O (5 mL). Then the two aqueous solutions were mixed and

$CuSO_4$ (64.0 mg, 0.26 mmol, 2eq) was added. The mixed solution was stirred for 0.5 h and the aqueous solution of NaOAc (0.1 g, 0.5 mmol, 4 eq) was added with stirring for another 3 days. The green cloudy solution was added with ion-exchange resin (Amberlite IR 15 TBA^+), which was synthesized according to the literature. Filtration gave a clear orange solution. Most of water in the solution was removed under reduced pressure and the addition of ethyl acetate gave 0.28 g of orange solid product in yield of 93.1%. ^{1}H NMR (500 MHz, DMSO) δ (ppm)= 8.31 (s, 2H), 7.90 (s, 2H), 7.54 (s, 2H), 4.72 (s, 4H), 4.60-4.43 (m, 10H), 4.29 (s, 4H), 3.90 (s, 2H), 3.77 (s, 2H), 3.53 (d, 4H), 3.16 (t, 24H), 3.06 (s, 2H), 2.70(s, 4H), 2.31(s, 4H), 1.57 (m, 24H), 1.31 (m, 24H), 0.94 (m, 36H).

$(Na)_3\{MnMo_6O_{18}[(OCH_2)_3CNHCO(CH_2)_2CONHCH_2(C_9H_{16}O_6N_3)]_2\}$ (SMMM). TMMM (1.2 g, 0.46 mmol) dissolving in CH_3CN (5 mL) was added dropwise into a vigorously stirred CH_3CN solution (5 mL) with $NaClO_4$ (5.7 g, 4.6 mmol). Then, the solution was stirred overnight to give an orange precipitate. Washing the precipitate twice with acetonitrile gave 0.89 g of the product SMMM in yield of 96.9%. ^{1}H NMR (500 MHz, DMSO) δ (ppm)= 8.31 (s, 2H), 7.90 (s, 2H), 7.54 (s, 2H), 4.73 (s, 4H), 4.61-4.45 (m, 10H), 4.29 (s, 4H), 3.91 (s, 2H), 3.77 (s, 2H), 3.53 (d, 4H), 3.06 (s, 2H), 2.70 (s, 4H), 2.31 (s, 4H), as shown in Figure S1. ^{13}C NMR ($CDCl_3$, 500MHz, 298 K) (ppm)= 123.84, 100.14, 74.52, 71.21, 70.46, 67.21, 65.34, 61.57, 49.77, 34.87, 31.83, 29.56, as shown in Figure S2. ESI-MS (m/z): (H^+) $[MnMo_6O_{24}]$ $(C_{38}H_{60}O_{16}N_{10})^{2-}$ ($HMMM^{2-}$): 964.2, found: 963.8, $[MnMo_6O_{24}]$ $(C_{38}H_{60}O_{16}N_{10})^{3-}$ (MMM^{3-}): 642.5, found: 642.6. as shown in Figure S3. FT-IR (KBr pellet) in v (cm^{-1}): 3433, 3338, 3065−2800, 1660, 1552, 1432, 1334, 1223, 1135, 1112, 1056, 943, 919, 904, 670 and 569. Elemental analysis calcd. for $(Na)_3MnMo_6O_{24}C_{38}H_{60}O_{16}N_{10}\cdot 3H_2O$ (NMM, 2068.5 g/mol): C, 22.26%; H, 3.24%; N, 6.83%; Na, 3.36%; Mn, 2.68%; Mo, 28.07%; found: C, 21.98%; H, 3.49%; N, 6.71%; Na, 3.43%; Mn, 2.61%; Mo, 27.85%.

S5. Structural characterizations of ionic complex molecule SMMM.

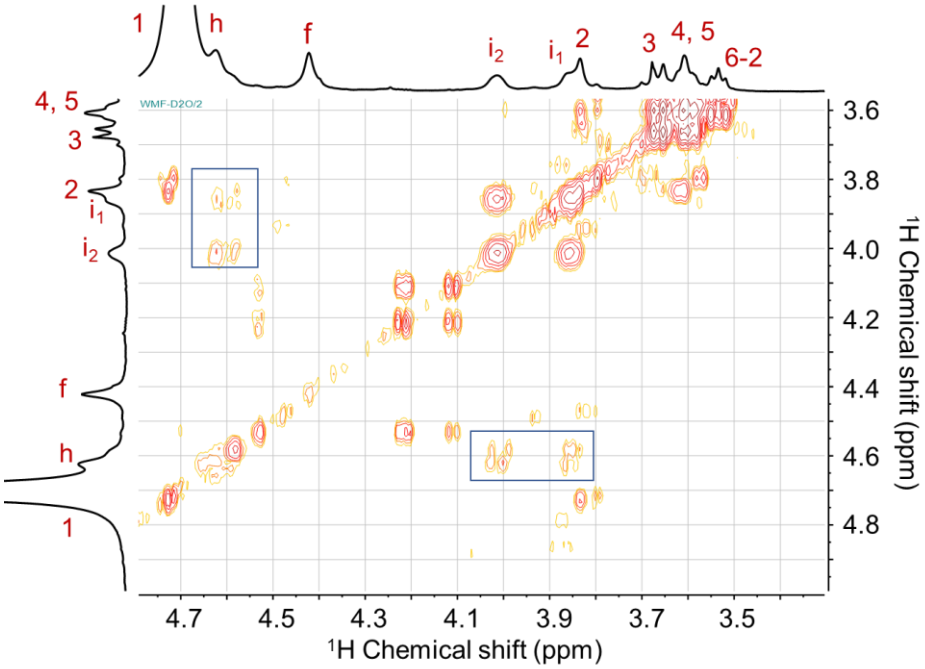

Fig. S2 ^{1}H NMR-2D COSY spectrum (D_2O, 500 MHz, 298 K) of SMMM.

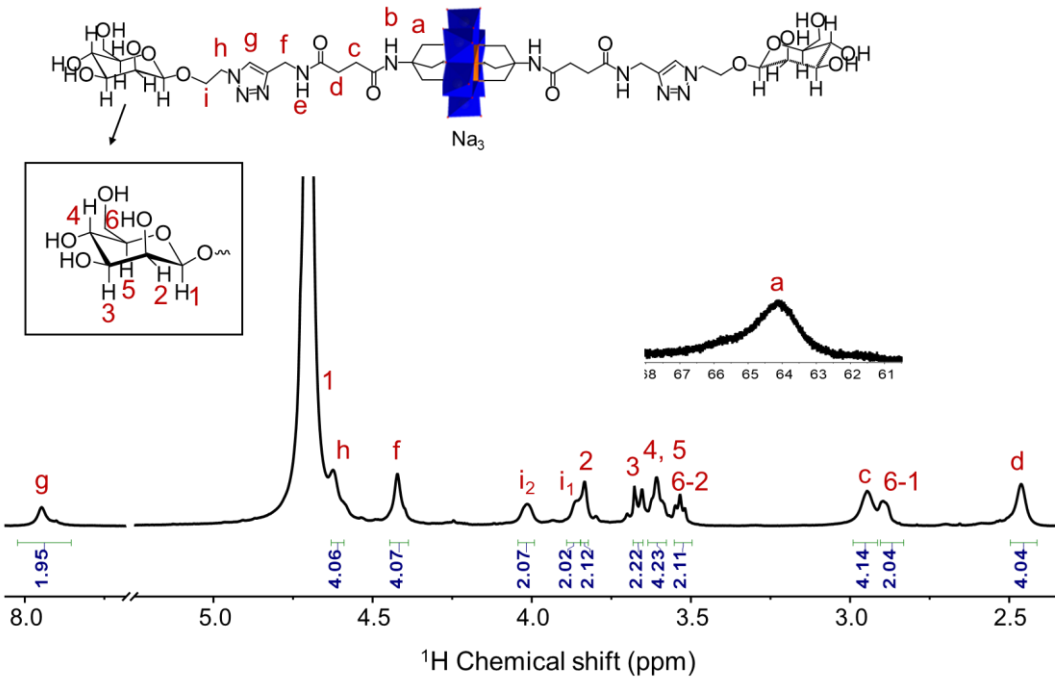

Fig. S3 ^{1}H NMR spectrum (D_2O, 500 MHz, 298 K) of SMMM.

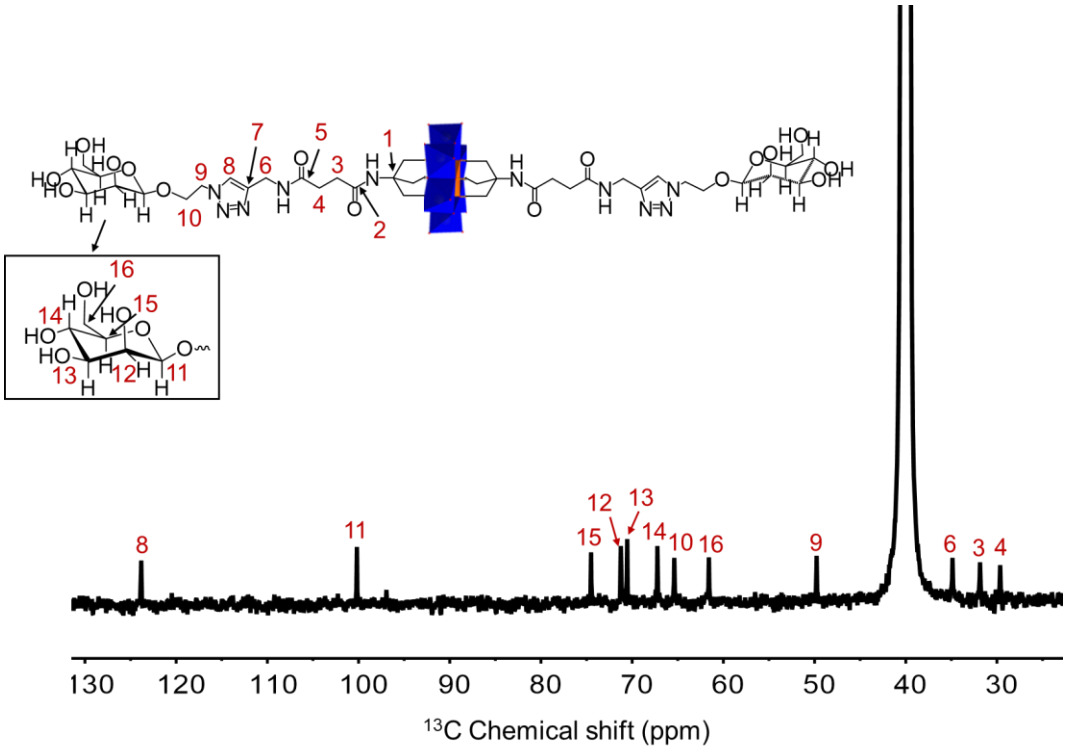

Fig. S4 ^{13}C NMR spectrum (DMSO, 500 MHz, 298 K) of SMMM.

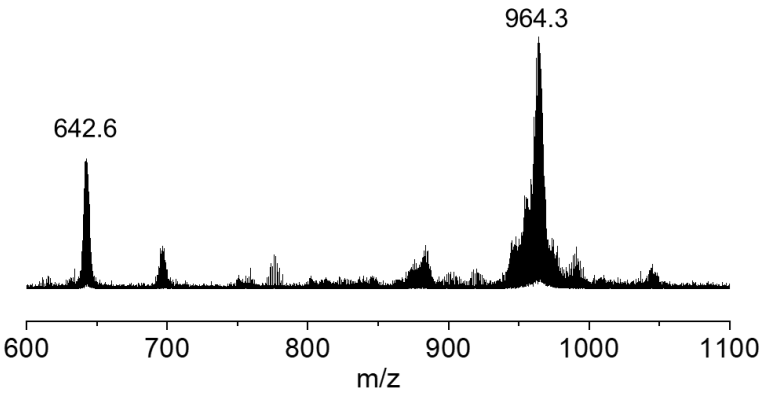

Fig. S5 ESI-MS spectrum of SMMM.

Table S1 Assignment to the ESI-MS spectrum of SMMM.

Chemical formula	Charge	MW* Calculated	MW Found
$(H^+)[MnMo_6O_{24}](C_{38}H_{60}O_{16}N_{10})^{2-}$	$2e^-$	964.2	963.8
$[MnMo_6O_{24}](C_{38}H_{60}O_{16}N_{10})^{3-}$	$3e^-$	642.5	642.6

*MW: Molecular weight.

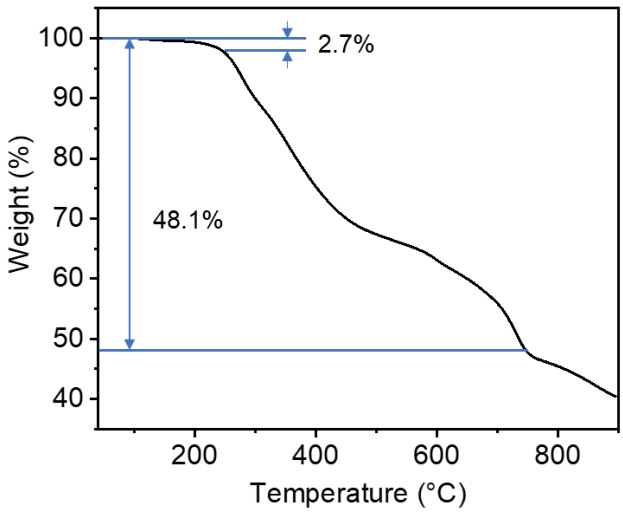

Fig. S6 TGA curve of SMMM.

Table S2 The ICP and organic elemental analysis of SMMM.

SMMM	N (%)	C (%)	H (%)	Na (%)	Mn (%)	Mo (%)
Found	6.71	21.98	3.49	3.43	2.61	27.85
Calculated	6.83	22.26	3.24	3.36	2.68	28.07

S6. Characterizations for the SMMM assemblies with different metal ions.

Table S3 The self-assembly of different metal ions and SMMM under sonication.

Monovalent metal ions (Alkali metals)	Li^+	LiCl	S
	Na^+	NaCl	S
	K^+	KCl	S
Divalent metal ions (Alkaline earth metals)	Mg^{2+}	$MgCl_2$	S
	Ca^{2+}	$CaCl_2$	S
	Ba^{2+}	$BaCl_2$	P
Divalent metal ions (Transition earth metals)	Mn^{2+}	$MnCl_2$	S
	Fe^{2+}	$FeCl_2$	G
	Co^{2+}	$CoCl_2$	G
	Ni^{2+}	$NiCl_2$	G
	Cu^{2+}	$CuCl_2$	G
	Zn^{2+}	$ZnCl_2$	S
Trivalent metal ions (Lanthanide series metals)	Eu^{3+}	$EuCl_3$	P
	Gd^{3+}	$GdCl_3$	P

S: Solution, G: hydrogel, P: Precipitate

Table S4 The self-assembly of different salts with metal ions and SMMM under sonication.

Divalent metal ions (Transition earth metals)	Fe^{2+}	$FeCl_2$	G
		$FeSO_4$	G
	Co^{2+}	$CoCl_2$	G
		$CoSO_4$	G
		$Co(OAc)_2$	G
		$Co(NO_3)_2$	G
	Ni^{2+}	$NiCl_2$	G
		$NiSO_4$	G
	Cu^{2+}	$CuCl_2$	G
		$CuSO_4$	G
		$Cu(OAc)_2$	G

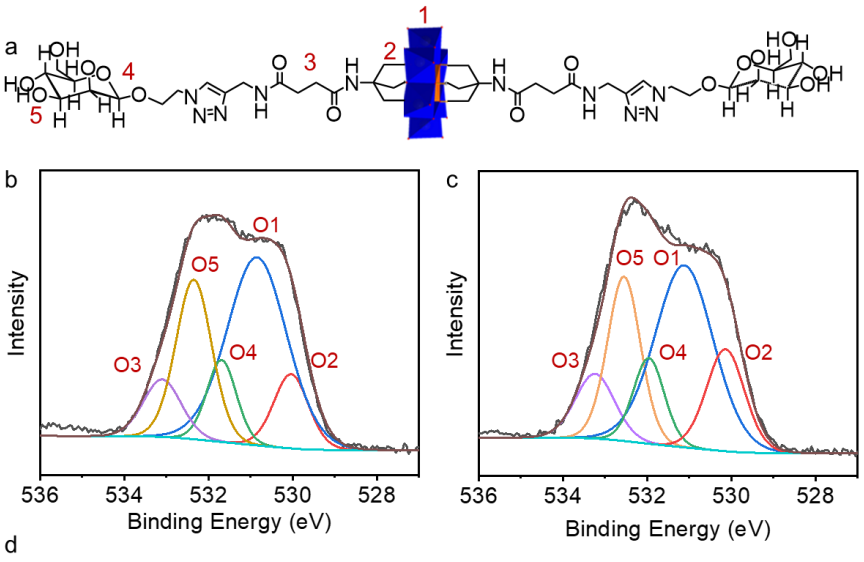

d

	O1	O2	O3	O4	O5
SMMM/eV	530.85	530.04	533.10	531.69	532.35
Co-gel/eV	531.12	530.14	533.24	531.96	532.55
Δ	0.27	0.10	0.14	0.27	0.20

Fig. S7 (a) Schematic diagram of SMMM molecular structure. XPS spectra of O1s for SMMM (b) and Co-gel (c), and corresponding O1s binding energy (d).

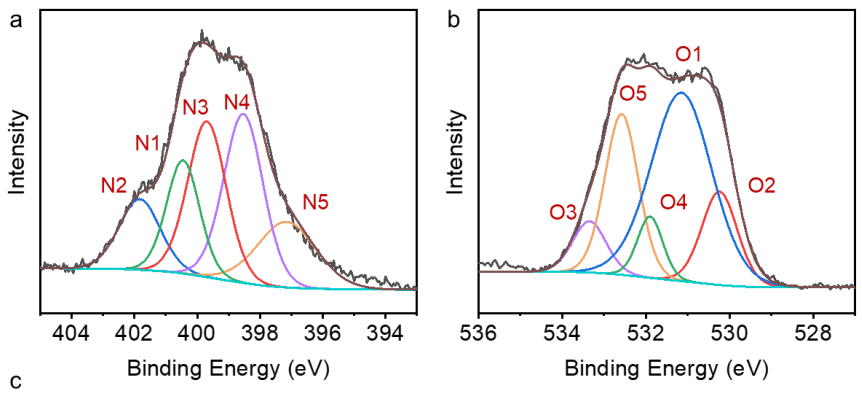

c

N1s/eV	**N1**	**N2**	**N3**	**N4**	**N5**
	399.69	401.83	400.45	398.53	397.15
O1s/eV	**O1**	**O2**	**O3**	**O4**	**O5**
	531.15	530.24	533.35	531.90	532.58

Fig. S8 XPS spectra for Cu-gel of N1s(a) and O1s (b), and corresponding binding energy (c).

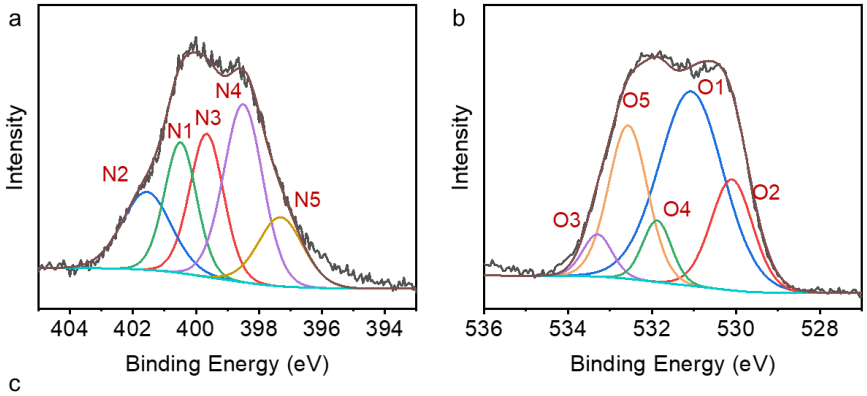

c

N1s/eV	**N1**	**N2**	**N3**	**N4**	**N5**
	399.66	401.56	400.49	398.50	397.31
O1s/eV	**O1**	**O2**	**O3**	**O4**	**O5**
	531.07	530.10	533.30	531.88	532.57

Fig. S9 XPS spectra for Fe-gel of N1s(a) and O1s (b), and corresponding binding energy (c).

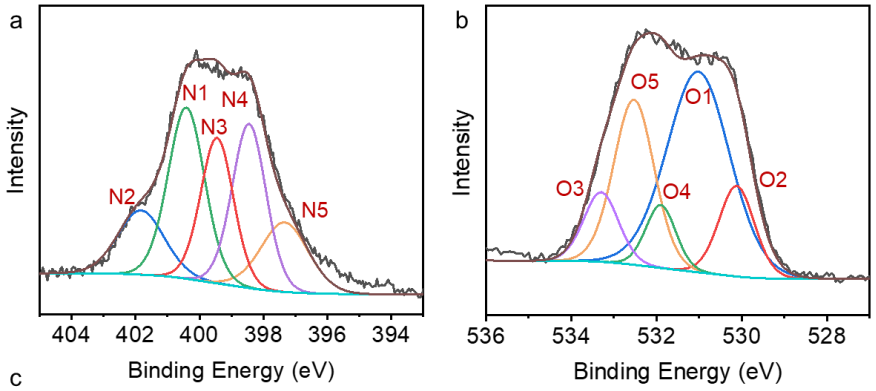

c

N1s/eV	N1	N2	N3	N4	N5
	399.45	401.83	400.41	398.45	397.34
O1s/eV	**O1**	**O2**	**O3**	**O4**	**O5**
	531.02	530.12	533.30	531.90	532.53

Fig. S10 XPS spectra for Ni-gel of N1s(a) and O1s (b), and corresponding binding energy (c).

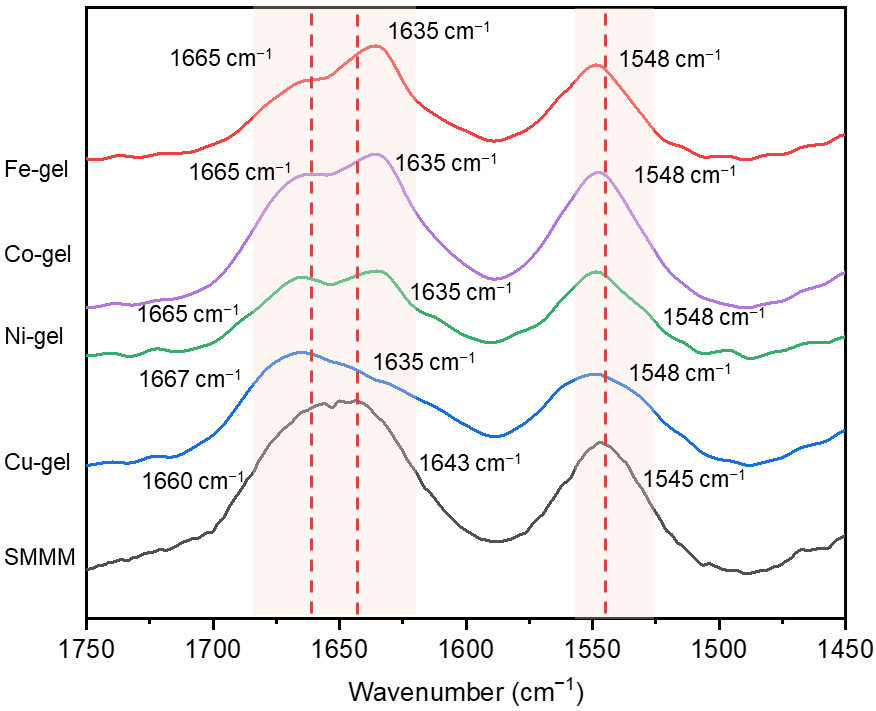

Fig. S11 FT-IR for SMMM and five hydrogels.

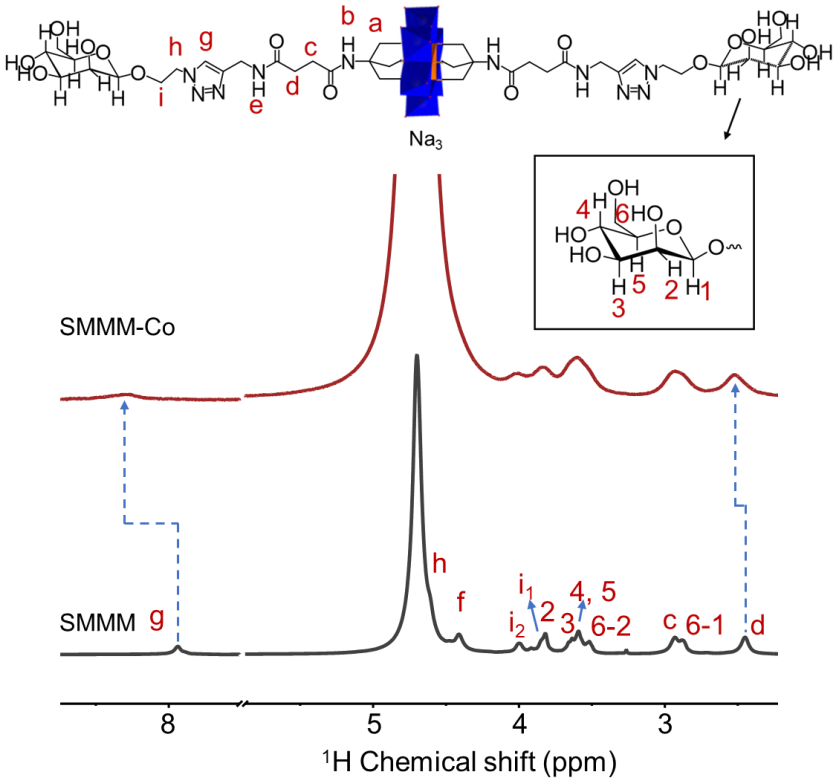

Fig. S12 ^{1}H NMR spectra of SMMM and inclusion Co^{2+} complex in D_2O.

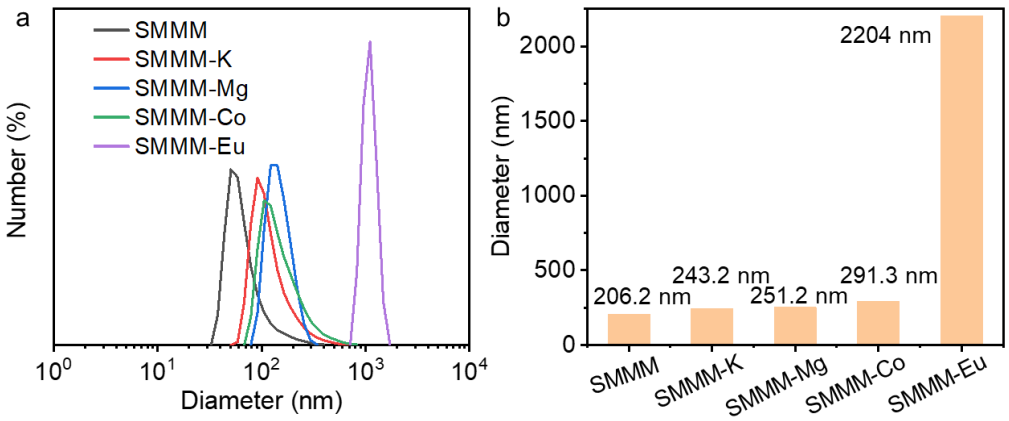

Fig. S13 SMMM assembly size distribution in water with different metal ions (a) and corresponding histogram (b).

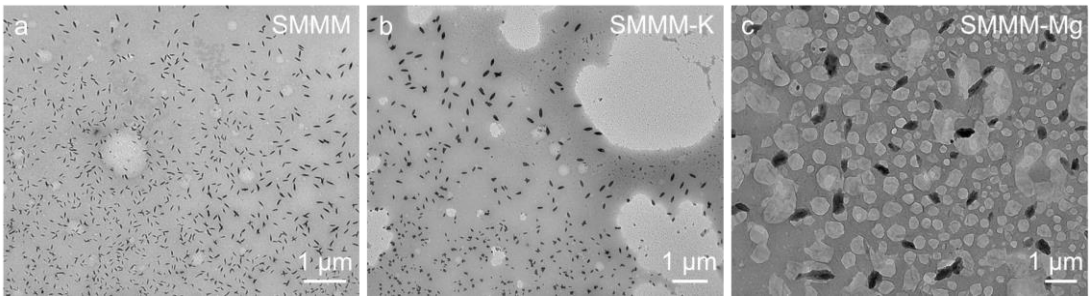

Fig. S14 (a–c) TEM images of SMMM assemblies with different metal ions.

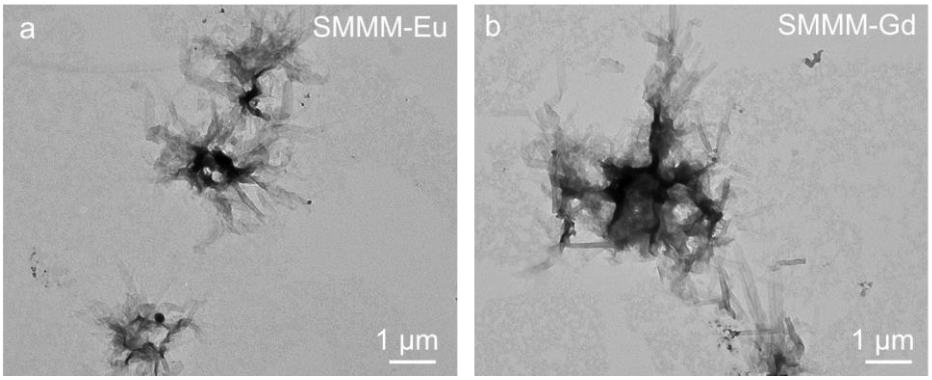

Fig. S15 TEM images of SMMM assemblies with Eu^{3+} (a) and Gd^{3+} (b).

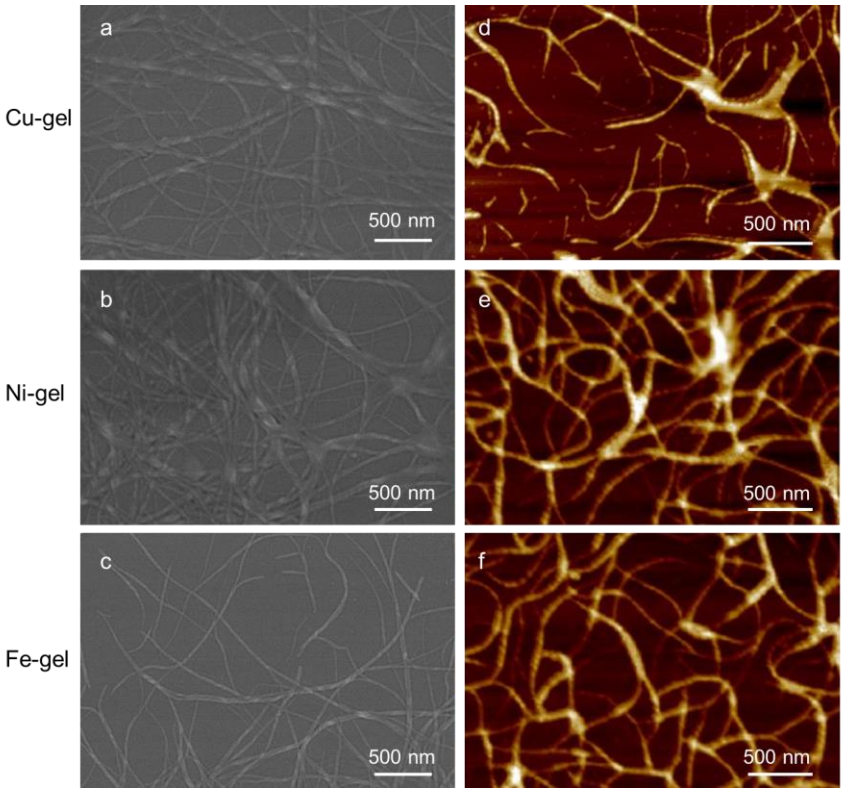

Fig. S16 SEM images (a–c) and AFM images (d–f) of Cu-gel, Ni-gel and Fe-gel.

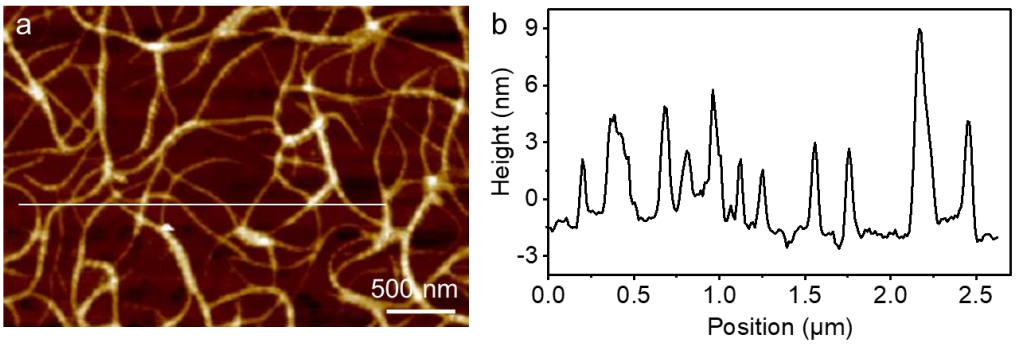

Fig. S17 (a) AFM image of Co-gel and (b) the height profile across the nanosheet in (a).

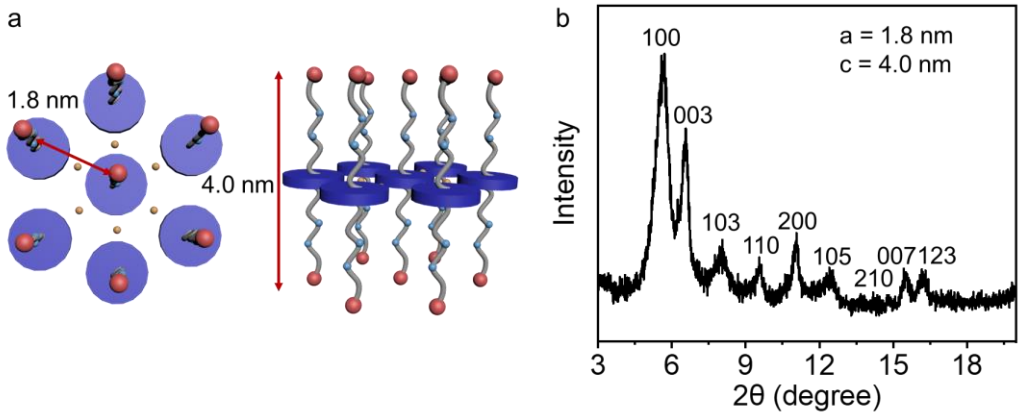

Fig. S18 (a, b) XRD pattern of the SMMM assembly and corresponding calculations of side spacing in plane and interlayer distance from XRD.

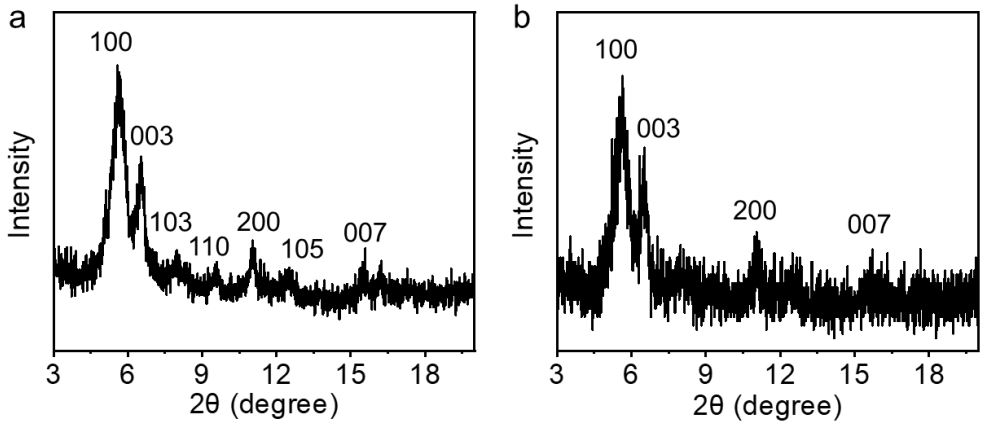

Fig. S19 XRD pattern of the SMMM with K^+ assembly (a) and Mg^{2+} assembly (b).

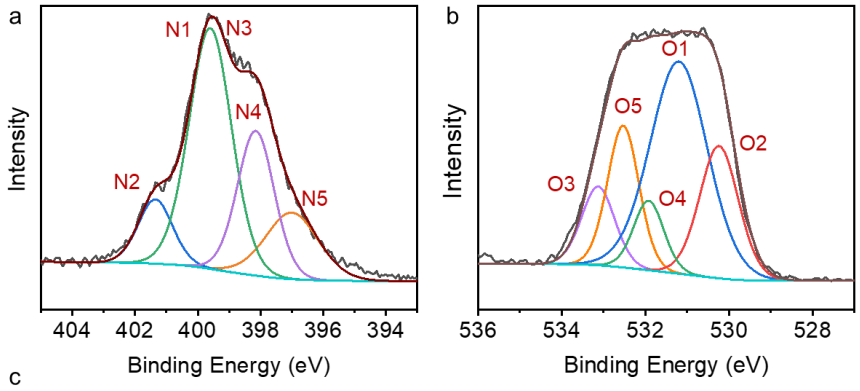

c

N1s/eV	**N1**	**N2**	**N3**	**N4**	**N5**
	399.6	401.35	399.6	398.15	397.0
O1s/eV	**O1**	**O2**	**O3**	**O4**	**O5**
	531.2	530.24	533.13	531.92	532.53

Fig. S20 XPS spectra for SMMM assembly with K^+ of N1s (a) and O1s (b), and corresponding binding energy (c).

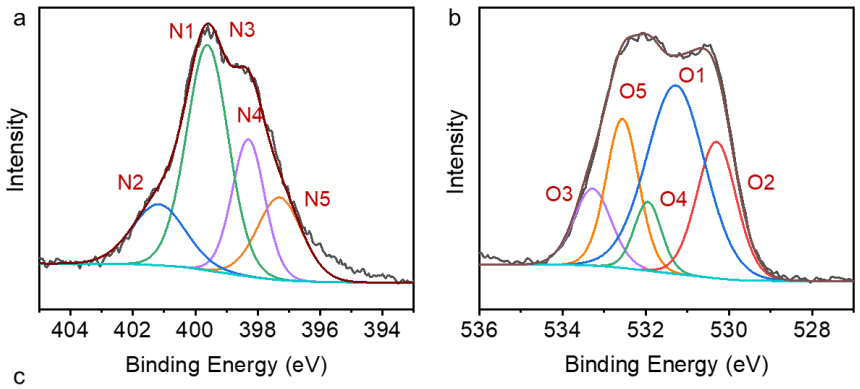

c

N1s/eV	**N1**	**N2**	**N3**	**N4**	**N5**
	399.61	401.17	399.61	398.3	397.3
O1s/eV	**O1**	**O2**	**O3**	**O4**	**O5**
	531.28	530.3	533.28	531.95	532.56

Fig. S21 XPS spectra for SMMM assembly with Mg^{2+} of N1s (a) and O1s (b), and corresponding binding energy (c).

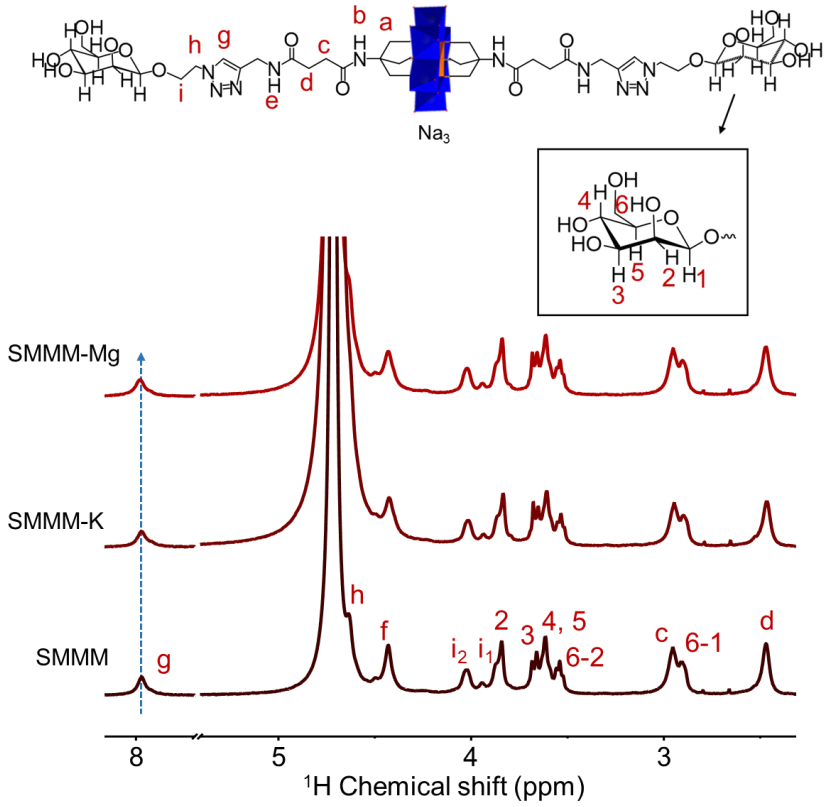

Fig. S22 ^{1}H NMR spectra of SMMM and inclusion K^{+} and Mg^{2+} complex in D_2O.

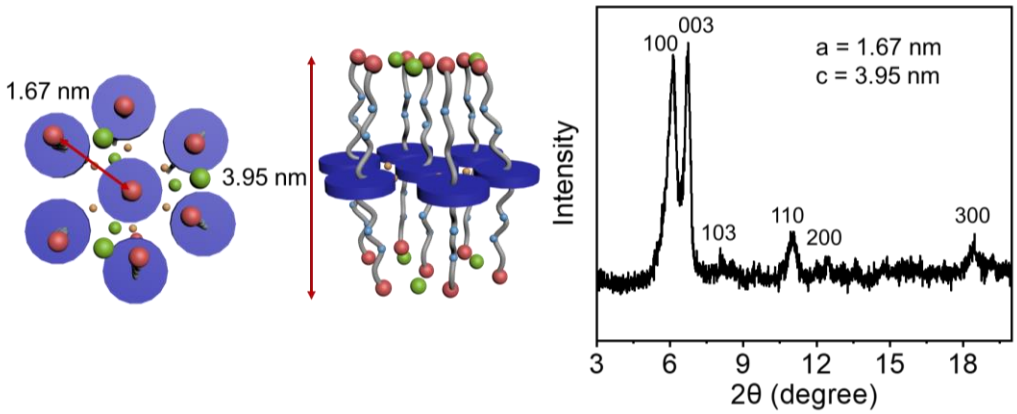

Fig. S23 (a, b) XRD pattern of the SMMM with Eu^{3+} assembly and corresponding calculations of side spacing in plane and interlayer distance from XRD.

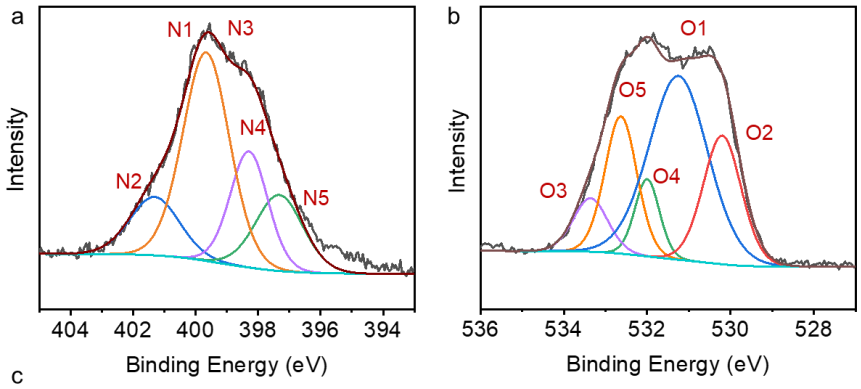

c

N1s/eV	**N1**	**N2**	**N3**	**N4**	**N5**
	399.66	401.31	399.66	398.29	397.32
O1s/eV	**O1**	**O2**	**O3**	**O4**	**O5**
	531.25	530.2	533.36	532.0	532.63

Fig. S24 XPS spectra for SMMM assembly with Gd^{3+} of N1s (a) and O1s (b), and corresponding binding energy (c).

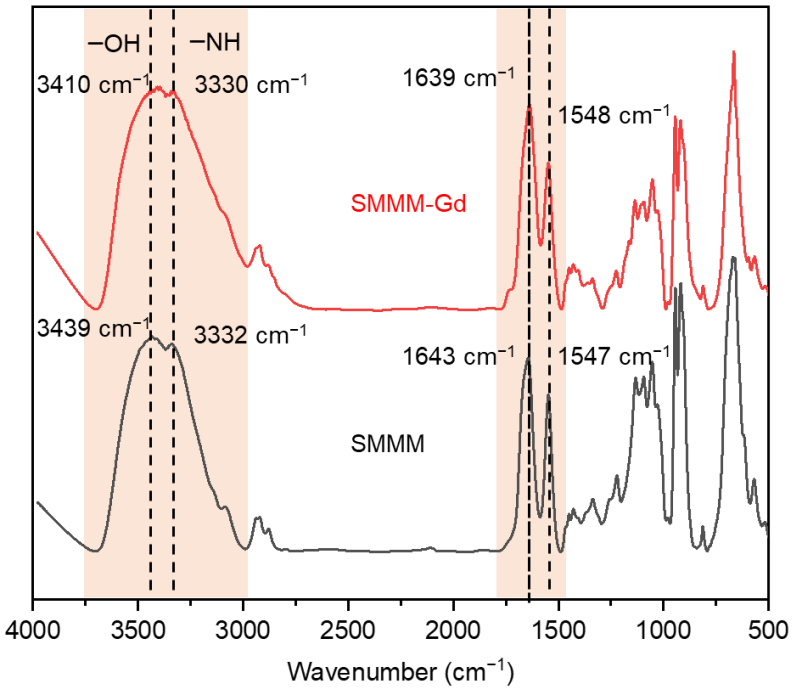

Fig. S25 FT-IR spectra of SMMM and inclusion Gd^{3+} complex.

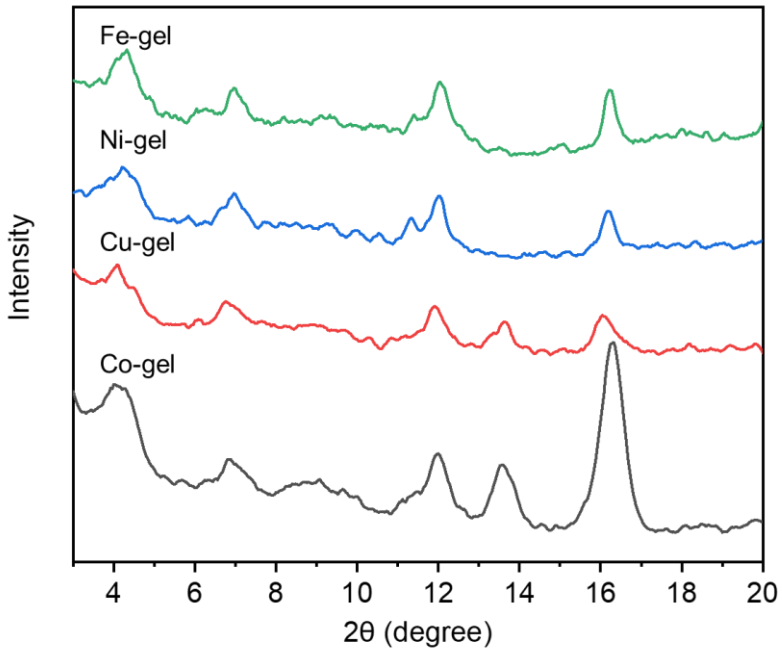

Fig. S26 XRD spectra of Co-gel, Cu-gel, Ni-gel and Fe-gel.

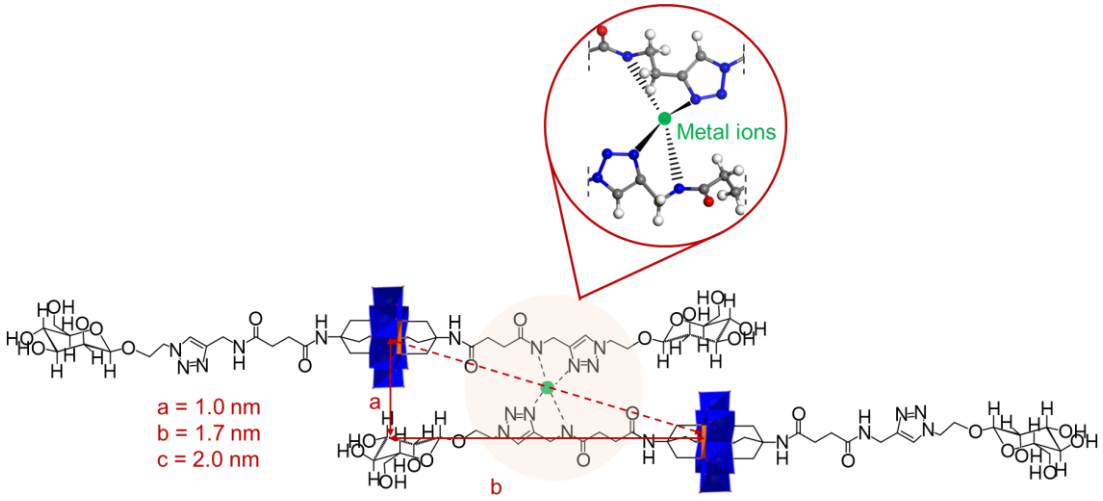

Fig. S27 The analysis of staggered structure and molecular size with SMMM and metal ions.

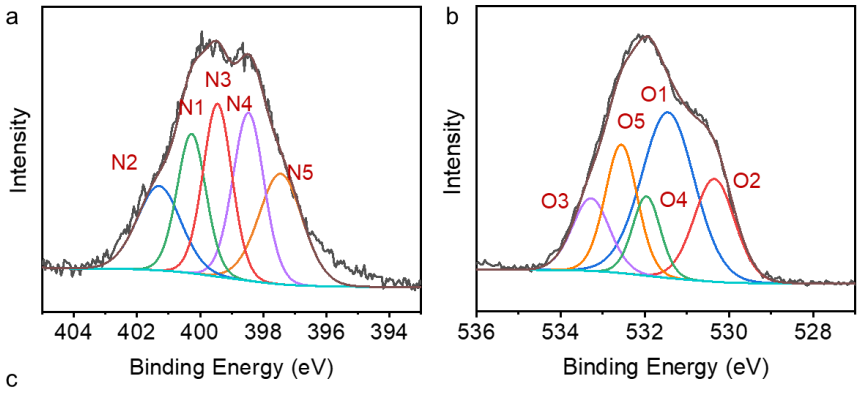

c

N1s/eV	**N1**	**N2**	**N3**	**N4**	**N5**
	399.45	401.3	400.27	398.47	397.45
O1s/eV	**O1**	**O2**	**O3**	**O4**	**O5**
	531.45	530.35	533.28	531.96	532.56

Fig. S28 XPS spectra for SMMM assembly with Zn^{2+} of N1s (a) and O1s (b), and corresponding binding energy (c).

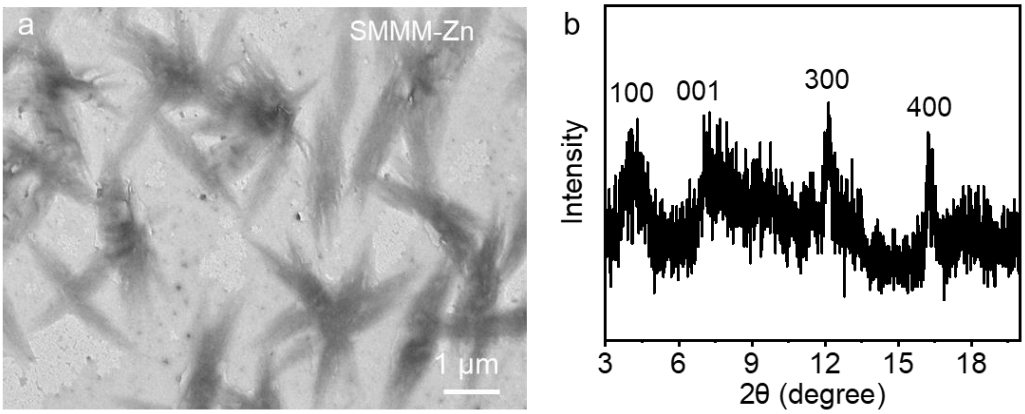

Fig. S29 TEM image of SMMM assemblies with Zn^{2+} (a) and XRD pattern (b).

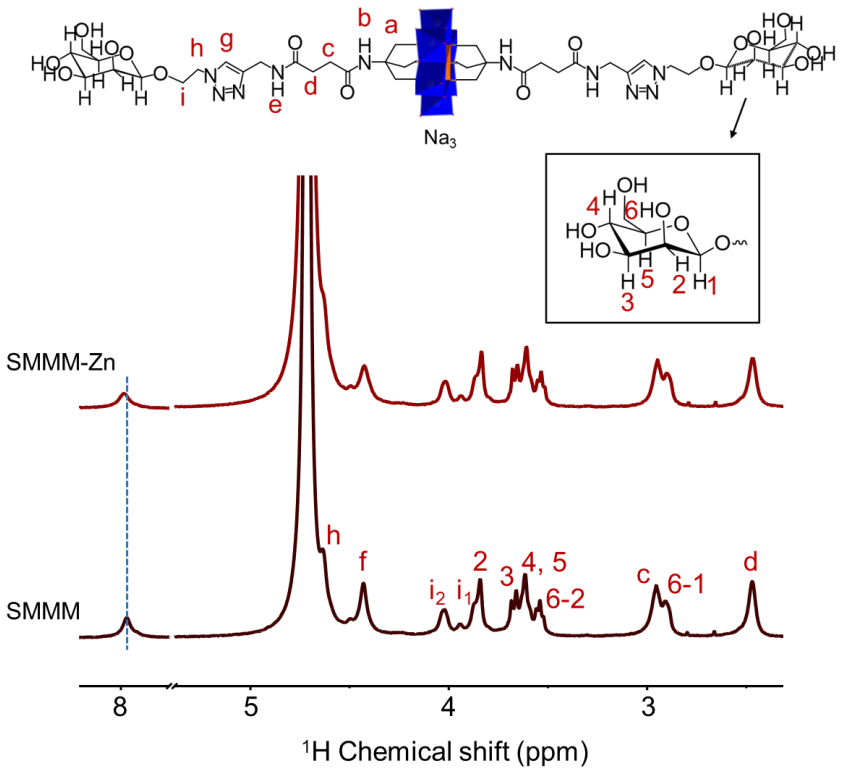

Fig. S30 ^{1}H NMR spectra of SMMM and inclusion Zn^{2+} complex in D_2O.

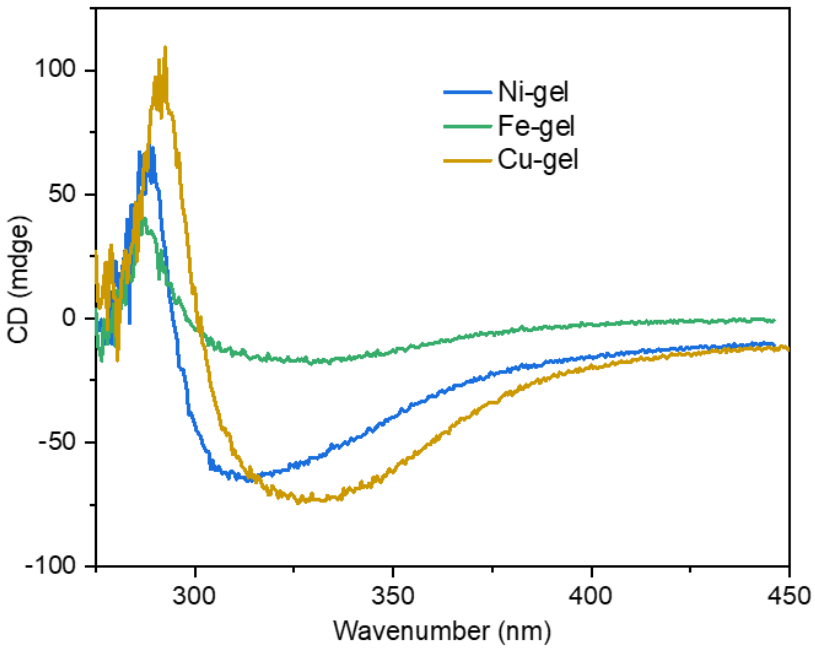

Fig. S31 CD spectra of Ni-gel, Fe-gel and Cu-gel.

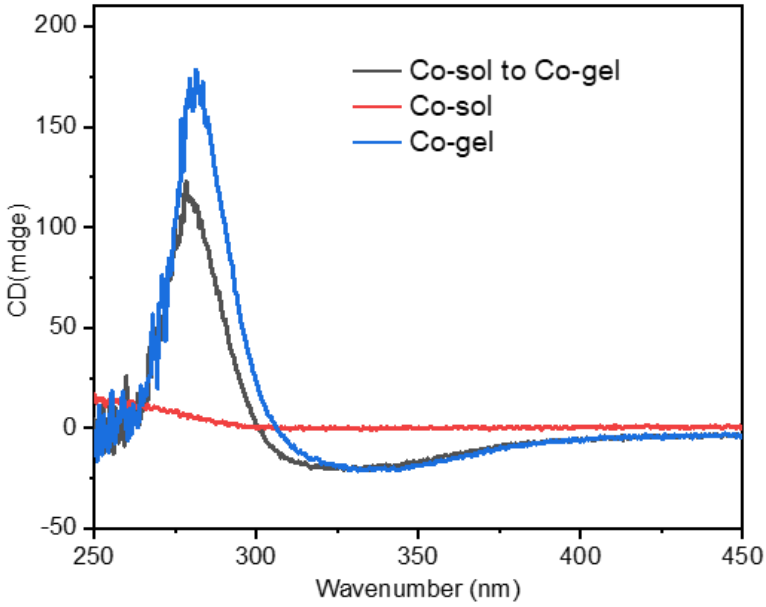

Fig. S32 CD spectra of Co-gel, Co-sol after heating and then sonication to get Co-gel.

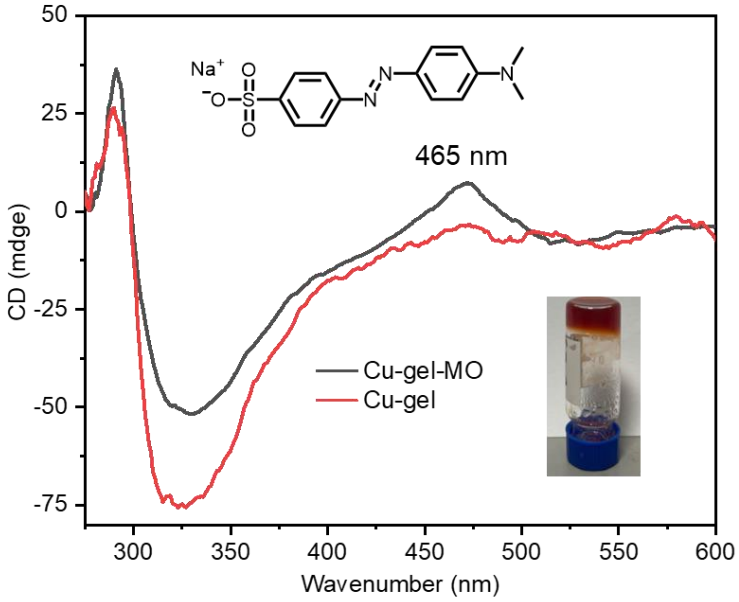

Fig. S33 CD spectra of Cu-gel, and adding methyl orange molecules.

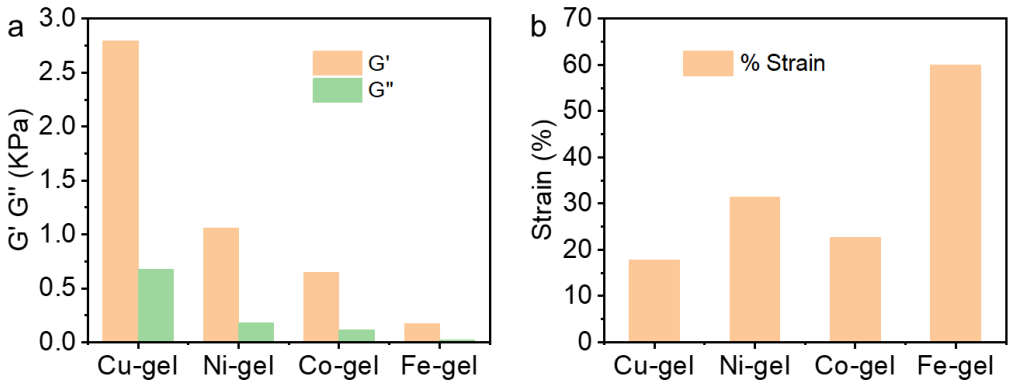

Fig. S34 (a) The modulus statistics graph of Rheology (frequency sweeps) and (b) the strain (%) statistics graph of Rheological analysis for supramolecular hydrogels.

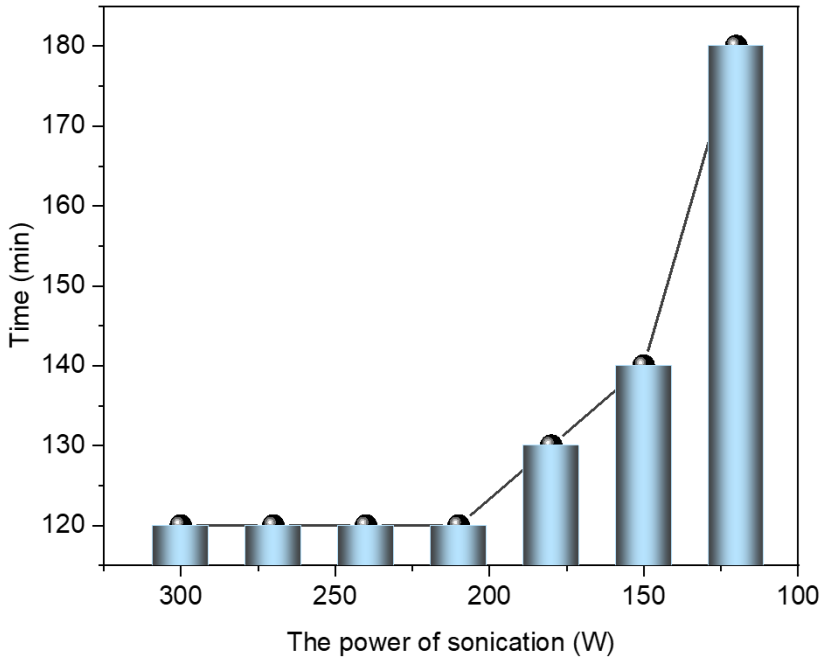

Fig. S35 The diagram of hydrogel formation time at different sonication power.

S7. References

[1] A. Macdonell, N. A. Johnson, A. J. Surman, L. Cronin, *J. Am. Chem. Soc.*, 2015, **137**, 5662−5665.

[2] N. Trattnig, J. B. Farcet, P. Gritsch, A. Christler, R. Pantophlet, P. Kosma, *J. Org. Chem.*, 2017, **82**, 12346−12358.